Structure and Bonding of $Li_{1.42(5)}Pd_2Sn_{5.58(5)}$: A Lithium Intercalated Palladium Stannide

Puravankara Sreeraj, Rolf-Dieter Hoffmann, Zhiyun Wu, and Rainer Pöttgen*

Institut für Anorganische und Analytische Chemie, Sonderforschungsbereich 458, and NRW Graduate School of Chemistry, Universität Münster, Corrensstrasse 36, D-48149 Münster, Germany

Ulrich Häussermann

Department of Inorganic Chemistry, Stockholm University, 10691 Stockholm, Sweden

Received November 3, 2004. Revised Manuscript Received December 9, 2004

The ternary stannide $Li_{1.42(5)}Pd_2Sn_{5.58(5)}$ was synthesized from the elements by induction melting in a sealed tantalum tube in a water-cooled quartz sample chamber. $Li_{1.42(5)}Pd_2Sn_{5.58(5)}$ was characterized by X-ray powder and single-crystal diffraction: *P*4/*mbm*, $a = 662.61(7)$ pm, $c = 843.39(10)$ pm, $V = 0.3703$ nm^3, $Z = 4$, wR2 = 0.0388, 477 F^2 values, and 17 variable parameters. It crystallizes with a new structure type that is closely related to the slightly orthorhombically distorted binary stannide $PdSn_3$. The palladium atoms in $Li_{1.42(5)}Pd_2Sn_{5.58(5)}$ have a square antiprismatic tin coordination. The square antiprisms are condensed via common edges and faces forming $[Pd_2Sn_6]$ double layers in a simple stacking sequence which leaves square prismatic voids for the lithium atoms. Syntheses with different starting compositions always resulted in the same refined composition $Li_{1+x}Pd_2Sn_{6-x}$ ($x = 0.40-0.46$) for the single crystals investigated. The tin sites within the double layers reveal an appreciable amount of Sn/Li mixing for six crystals investigated, in agreement with EDX data. First principles electronic structure calculations were employed to analyze the bonding situation and the nature of the Sn/Li mixed occupancy in $Li_{1+x}Pd_2Sn_{6-x}$. It was found that by reducing the electron count of $LiPd_2Sn_6$, which can be achieved by a partial replacement of Sn by Li, the Fermi level is shifted to a dip in the density of states. This is a favorable situation and the corresponding electron count leads to a composition $Li_{1.45}Pd_2Sn_{5.65}$, which is very close to the experimentally found value. The location of this dip coincides with a turnover of Pd−Sn and Sn−Sn interactions from being bonding/nonbonding to being antibonding.

1. Introduction

The tin-rich binary and ternary stannides of the late transition metals (*T*) predominantly have a square antiprismatic coordination for the *T* atoms. These square antiprisms can be condensed in different ways leading to the various structure types observed. In the Ir_3Ge_7 type structure of Ru_3Sn_7[1−3] two prisms are condensed via a common square, and these double units condense via common tin corners, forming a three-dimensional network. In the stannides α-$CoSn_3$, β-$CoSn_3$,[4] $RhSn_2$, $PdSn_2$,[5] $PdSn_3$,[6] $IrSn_4$,[7] and $PdSn_4$,[8] the square antiprisms are condensed via common edges or via common edges and common square faces, leading to two-dimensional building blocks which are interconnected via Sn−Sn bonds. An overview on the different connectivities is given in a recent publication.[6]

The cubic stannides with the Ir_3Ge_7 type structure show significant solid solubility: $Rh_3Sn_{7-x}Mg_x$[9] and $Ir_3Sn_{7-x}Mg_x$.[10] Magnesium atoms substitute tin atoms in the covalently bonded network. Recent investigations in the related lithium-based systems revaled that lithium as well can substitute tin and form solid solutions $Rh_3Sn_{7-x}Li_x$ and $Ir_3Sn_{7-x}Li_x$.[11] In contrast, the lithium atoms in $LiTSn_4$ (T = Ru, Rh, Ir)[12,13] and $LiCoSn_6$[14] occupy proper sites with a slightly stuffed cubic tin environment. When searching for similar intermetallic compounds in the lithium−palladium−tin system we observed the phases $Li_{1+x}Pd_2Sn_{6-x}$ ($x = 0.40-0.46$) with a peculiar crystal chemistry. The refined composition of different crystals was always close to $Li_{1.42(5)}Pd_2Sn_{5.58(5)}$. Herein we report on the synthesis, the crystal chemistry, and a chemical bonding analysis of the $Li_{1+x}Pd_2Sn_{6-x}$ series. A

* To whom correspondence should be addressed. E-mail: pottgen@uni-muenster.de.

(1) Nial, O. *Sven. Kem. Tidskr*. **1947**, *59*, 172.
(2) Chakoumakos, B. C.; Mandrus, D. *J. Alloys Compd*. **1998**, *281*, 157.
(3) Eriksson, L.; Lanner, J. *Acta Crystallogr*. **2001**, *E57*, i85.
(4) Lang, A.; Jeitschko, W. *Z. Metallkd*. **1996**, *87*, 759.
(5) Hellner, E. *Z. Kristallogr*. **1956**, *107*, 99.
(6) Nylén, J.; Garcia Garcia, F. J.; Mosel, B. D.; Pöttgen, R.; Häussermann, U. *Solid State Sci*. **2004**, *6*, 147.
(7) Nordmark, E.-L.; Wallner, O.; Häussermann, U. *J. Solid State Chem*. **2002**, *168*, 34.
(8) Künnen, B.; Niepmann, D.; Jeitschko, W. *J. Alloys Compd*. **2000**, *309*, 1.
(9) Schlüter, M.; Kunst, A.; Pöttgen, R. *Z. Anorg. Allg. Chem*. **2002**, *628*, 2641.
(10) Schlüter, M.; Häussermann, U.; Heying, B.; Pöttgen, R. *J. Solid State Chem*. **2003**, *173*, 418.
(11) Kurowski, D.; Hoffmann, R.-D.; Wu, Zh.; Pöttgen, R.; Häussermann, U., unpublished results.
(12) Wu, Zh.; Hoffmann, R.-D.; Pöttgen, R. *Z. Anorg. Allg. Chem*. **2002**, *628*, 1484.
(13) Wu, Zh.; Eckert, H.; Senker, J.; Johrendt, D.; Kotzyba, G.; Mosel, B. D.; Trill, H.; Hoffmann, R.-D.; Pöttgen, R. *J. Phys. Chem. B* **2003**, *107*, 1943.
(14) Pöttgen, R.; Wu, Zh.; Hoffmann, R.-D.; Kotzyba, G.; Trill, H.; Senker, J.; Johrendt, D.; Mosel, B. D.; Eckert, H. *Heteroatom Chem*. **2002**, *13*, 506.

10.1021/cm0401995 CCC: $30.25
Published on Web 01/29/2005

Table 1. Crystal Data Refinement and Lattice Parameters (pm) for Several Lithium Palladium Stannides $Li_{1+x}Pd_2Sn_{6-x}$; Refined R and *w*R Factors Shown below Are for the 4σ Data[a]

starting composition (Li/Pd/Sn)	refined composition	*a*/pm	*c*/pm	F(000)	R_1	*w*R2
0.25:2:5.75	$Li_{1.46}Pd_2Sn_{5.54}$	663.31(9)	842.78(17)	746.8	0.0184	0.0391
0.50:2:5.50	$Li_{1.41}Pd_2Sn_{5.59}$	663.08(9)	843.19(17)	751.5	0.0226	0.0479
0.75:2:5.25	$Li_{1.40}Pd_2Sn_{5.60}$	663.19(7)	844.75(10)	752.4	0.0349	0.0612
1.00:2:6.00	$Li_{1.43}Pd_2Sn_{5.57}$	663.92(9)	843.19(17)	749.6	0.0296	0.0614
1.40:2:5.60	$Li_{1.43}Pd_2Sn_{5.57}$	662.98(7)	842.99(10)	750.1	0.0302	0.0731
1.50:2:4.50	$Li_{1.42}Pd_2Sn_{5.58}$	662.61(7)	843.39(10)	751	0.0196	0.0388

[a]The refined compositions are the same within the combined standard deviations (see Table 2).

preliminary account of some results was given recently at a conference.[15]

2. Experimental Procedures

2.1 Syntheses. Starting materials for the syntheses of the stannides with the nominal compositions $(1 + x)$:2:$(6 - x)$ Li/Pd/Sn ($x = 0.25$, 0.5, 0.75, 1.0, 1.4, and 1.5) were lithium rods (Merck, >99%), palladium powder (Degussa-Hüls, ~200 mesh, 99.9%), and tin granules (Merck, 99.9%). The lithium rods were cut into smaller pieces under dry paraffin oil and subsequently washed with *n*-hexane. The paraffin oil and *n*-hexane were dried over sodium wire. The lithium pieces were kept in Schlenk tubes under argon prior to the reactions. Argon was purified over a titanium sponge (900 K), silica gel, and molecular sieves.

The lithium pieces were mixed with palladium powder and tin granules in the ideal atomic ratio for different starting compositions (Table 1) under flowing argon, and then sealed in a tantalum ampule under an argon pressure of about 800 mbar in an arc-melting apparatus.[16] The tantalum tube was subsequently enclosed in an evacuated silica tube for oxidation protection. Subsequently the samples were rapidly heated to 970 K and held at this temperature for 5 h. The temperature was then lowered to 670 K and kept at this temperature for 2 days, followed by quenching in sand.

No single crystals suitable for structure determination were obtained in the annealing step mentioned above. Crystal growth was performed applying a special temperature mode. A new reaction mixture was therefore first heated to 520 K, at a rate of 0.2 K/min, to melt Li and Sn. Subsequently, the temperature was slowly increased to 920 K and held at that temperature for 24 h. The sample was slowly cooled over 50 h to 620 K, and annealed for 3 days. Finally, the ampule was slowly cooled to 373 K over 42 h. The sample could be readily separated from the tantalum tube. No reaction with the container material was observed. The polycrystals and single crystals exhibited metallic luster, whereas powders were dark gray. All stannides prepared were stable in air over several weeks.

2.2 EDX Analyses. The single crystals investigated on the diffractometers were analyzed with a Leica 420 I scanning electron microscope. The EDX analyses were carried out with elemental palladium and tin as standards. Neither metallic impurities nor tantalum contaminants from the crucible were detected. The Pd/Sn ratios determined from different measurements on all crystals varied between 1:2.66 and 1:2.78, in good agreement with the refined compositions (Table 3) which varied between 2.77 and 2.80. The small uncertainties in the EDX data are due to the irregular surface of the small single crystals.

2.3 X-ray Investigations. The samples were characterized through their Guinier powder patterns using Cu Kα_1 radiation and α-quartz ($a = 491.30$ pm, $c = 540.46$ pm) as an internal standard.

Table 2. Crystal Data and Structure Refinement for $Li_{1.42(5)}Pd_2Sn_{5.58(5)}$

empirical formula	$Li_{1.42(5)}Pd_2Sn_{5.58(5)}$
molar mass (g/mol)	442.75
unit cell dimensions	$a = 662.61(7)$ pm
(Guinier powder data)	$c = 843.39(10)$ pm
	$V = 0.3703$ nm^3
formula units per cell	$Z = 4$
calculated density	7.94 g/cm^3
crystal size	$20 \times 45 \times 65$ μm^3
transmission (max/min)	1.10
absorption coefficient	23.1 mm^{-1}
$F(000)$	751
θ range for data collection	2° to 35°
range in *hkl*	±10; ±10; ±13
total no. of reflections	5471
independent reflections	477 ($R_{int} = 0.0450$)
reflections with $I > 2\sigma(I)$	419 ($R_{sigma} = 0.0174$)
data/parameters	477/17
goodness-of-fit on F^2	1.074
final *R* indices [$I > 2\sigma(I)$]	$R_1 = 0.0195$
	$wR_2 = 0.0378$
R indices (all data)	$R_1 = 0.0252$
	$wR_2 = 0.0388$
extinction coefficient	0.0085(4)
largest diff. peak and hole	0.77 and −1.79 e/Å^3

The Guinier camera was equipped with an imaging plate detector (Fujifilm, Basread-1800). To ensure correct indexing, the observed patterns were compared with calculated ones[17] taking the positions of the refined structures. The refined lattice parameters are listed in Table 1. The lattice parameters derived from the single-crystal diffractometer and those refined from the powders agreed well.

Small regularly shaped single crystals of the samples $(1 + x)$:2:$(6 - x)$ Li/Pd/Sn ($x = 0.25$, 0.5, 0.75, 1.0, 1.4, and 1.5) were isolated from the annealed specimens. They were investigated on a Buerger precession camera equipped with an imaging plate system (Fujifilm BAS-1800) to establish both symmetry and suitability for intensity data collection.

Intensity data of suitable single crystals were recorded at room temperature by use of a four-circle diffractometer (CAD4) with graphite monochromatized Mo Kα radiation ($\lambda = 71.073$ pm) and a scintillation counter with pulse-height discrimination. The scans were taken in the $\omega/2\theta$ mode. Empirical absorption corrections were applied on the basis of psi-scan data, followed by a spherical absorption correction. Three of the crystals were investigated in the oscillation mode on a Stoe image plate system (IPDS-II) with graphite monochromatized Mo Kα radiation. Numerical absorption corrections were applied to these data. As an example, all relevant crystallographic data and details for the data collection and evaluation for the stannide with the refined composition $Li_{1.42(5)}Pd_2Sn_{5.58(5)}$ (staring composition 1.5:2:4.5 Li/Pd/Sn) are listed in Table 2.

Analysis of the diffraction data revealed that all samples crystallize with a tetragonal structure, space group *P4/mbm*. The

(15) Sreeraj, P.; Hoffmann, R.-D.; Pöttgen, R. *Z. Anorg. Allg. Chem.* **2004**, *630*, 1761.
(16) Pöttgen, R.; Gulden, T.; Simon, A. *GIT Labor-Fachz.* **1999**, *43*, 133.
(17) Yvon, K.; Jeitschko, W.; Parthé, E. *J. Appl. Crystallogr.* **1977**, *10*, 73.

Table 3. Refined Compositions and *M* (Sn2/Li2) Site Occupancy Parameters for the Stannides $Li_{1+x}Pd_2Sn_{6-x}$ ($x = 0.40-0.46$) from Single Crystal Data

starting composition (Li/Pd/Sn)	refined compositon	occup./%
0.25:2:5.75	$Li_{1.46}Pd_2Sn_{5.54}$	77.4(1) Sn2/22.6(1) Li2
0.50:2:5.50	$Li_{1.41}Pd_2Sn_{5.59}$	78.7(1) Sn2/21.3(1) Li2
0.75:2:5.25	$Li_{1.40}Pd_2Sn_{5.60}$	79.7(1) Sn2/20.3(1) Li2
1.00:2:6.00	$Li_{1.43}Pd_2Sn_{5.57}$	78.6(2) Sn2/21.4(2) Li2
1.40:2:5.60	$Li_{1.43}Pd_2Sn_{5.57}$	78.3(1) Sn2/21.7(1) Li2
1.50:2:4.50	$Li_{1.42}Pd_2Sn_{5.58}$	79.0(1) Sn2/21.0(1) Li2

starting atomic positions were deduced from automatic interpretations of direct methods with SHELXS-97.[18] The structures were then refined with SHELXL-97[19] with anisotropic displacement parameters for the palladium and tin sites. The lithium sites were obtained from a difference Fourier synthesis and these sites were refined with isotropic displacement parameters. As a check for the correct compositions and site assignments (palladium and tin differ only by four electrons), the occupancy parameters of palladium and tin were refined in a separate series of least-squares cycles. The Pd and Sn1 sites were fully occupied within two standard deviations, while all Sn2 sites of the six investigated crystals showed a lower occupancy. At first sight one might think of palladium/tin mixing for these sites, however, the scattering power observed for these positions is even less than that for full palladium occupancy. Pd/Li mixing would lead to unreasonably short Pd−Pd distances. In agreement with the Pd/Sn ratios determined by EDX, these sites have then been refined with Sn/Li mixing, leading to the refined compositions listed in Table 3.

In the final cycles, the ideal occupancies were assumed again for Li, Pd, and Sn1, while the mixed Li2/Sn2 occupancy has been refined as a least-squares variable. Subsequent difference Fourier syntheses revealed no significant residual peaks. The positional parameters determined for the six refinements were almost the same. As an example we list the positional parameters and interatomic distances for the stannide $Li_{1.42(5)}Pd_2Sn_{5.58(5)}$ (starting composition 1.5:2:4.5 Li/Pd/Sn) in Tables 4 and 5. Further details on the structure refinement of $Li_{1.42(5)}Pd_2Sn_{5.58(5)}$ are available.[20]

2.4 Electronic Structure Calculations. Total energy calculations for ideal $LiPd_2Sn_6$ were performed in the framework of the frozen core all-electron projected augmented wave (PAW) method[21] (as implemented in the program VASP).[22] For all systems atomic position parameters and lattice parameters were relaxed for a set of constant volumes until forces had converged to less than 0.01 eV/Å. In a second step, we extracted the equilibrium volume V_0 and its corresponding energy E_0 by fitting the E vs V values to a Birch−Murnaghan equation of state. The exchange and correlation effects were treated within local density approximation (LDA) using the Ceperly−Alder functional.[23] Convergency of the calculations was checked with respect to the plane wave cutoff and the number of k points used in the summation over the Brillouin zone. Concerning the plane wave cutoff an energy value of 300 eV was chosen. The k points were generated by the Monkhorst−Pack method[24] and sampled on a grid of $10 \times 10 \times 10$. The integration over the Brillouin zone was performed with a Gaussian smearing of 20 mRy. Total energies were converged to better than 2 meV/atom.

The TB-LMTO method in the atomic sphere approximation[25] was employed to calculate crystal orbital Hamilton populations (COHP)[26] for $LiPd_2Sn_6$ and $PdSn_3$. A COHP analysis provides a measure of the bonding character and strength of atomic contacts. The TB-LMTO calculations were performed on the basis of the VASP−PAW relaxed structure. The electronic density of states (DOS) produced by both methods were found to be in good agreement.

Results and Discussion

Crystal Chemistry. The new stannide $Li_{1.42(5)}Pd_2Sn_{5.58(5)}$ reported herein belongs to a large structural family of intermetallics where Sn atoms form 3^2434 nets which sandwich layers of transition metal atoms in such a way that the latter attain a square antiprismatic coordination (i.e., α-$CoSn_3$, β-$CoSn_3$,[4] $PdSn_3$,[6] $IrSn_4$,[7] and $PdSn_4$[8]). The structures of these stannides can easily be related when regarding the TSn_8 layers as building blocks. First, a building block may consist of a single (composition TSn_4) or double layer of TSn_8 square antiprisms (composition TSn_3). Second, building blocks are mutually shifted and may be stacked in an $A_{(0,0)}B_{(1/2,0)}A_{(0,0)}B_{(1/2,0)}$ or $A_{(0,0)}B_{(1/2,0)}C_{(1/2,1/2)}D_{(0,1/2)}$ fashion where the subscripts denote the relative shift vector with respect to the reference building block A. The building principle of tin-rich transition metal intermetallics has been introduced and explained in detail in our previous works on $PdSn_n$ ($n = 2,3,4$),[6] $IrSn_4$,[7] and $(Co,Ni)Sn_2$.[27]

As emphasized in Figure 1, the structure of $Li_{1.42(5)}Pd_2Sn_{5.58(5)}$ derives from that of binary $PdSn_3$. The latter represents a stacking of double layers of $PdSn_8$ square antiprisms and these double layer building blocks simply appear intercalated by Li in $Li_{1.42(5)}Pd_2Sn_{5.58(5)}$. However, there is a distinct difference between the arrangements of the Pd_2Sn_6 blocks in both structures. According to the terminology introduced in ref 27 the stacking sequence of blocks is $A_{(0,0)}B_{(1/2,0)}A_{(0,0)}B_{(1/2,0)}$ in $PdSn_3$ whereas in $Li_{1.42(5)}Pd_2Sn_{5.58(5)}$ it is $A_{(0,0)}C_{(1/2,1/2)}A_{(0,0)}C_{(1/2,1/2)}$. The AC orientation between adjacent building blocks Pd_2Sn_6 results in a square-prismatic Sn coordination for the intercalating lithium atoms. This coordination also occurs in the lithium stannides $LiTSn_4$ (T = Ru, Rh, Ir),[12] and $LiCoSn_6$.[14] For detailed drawings of these stacking sequences we refer to previous work.[6,27]

Now it is interesting to discuss the structural changes that occur upon lithium incorporation into $PdSn_3$. The most obvious change is the crystal system. $PdSn_3$ is orthorhombic, space group *Cmca*, $a = 1714.7(6)$, $b = 645.8(3)$, $c = 648.8(2)$ pm, while the $Li_{1.42(5)}Pd_2Sn_{5.58(5)}$ stannide is tetragonal, space group *P*4/*mbm* with the lattice parameters $a = 662.61(7)$, $c = 843.39(10)$ pm. In the ternary stannides

(18) Sheldrick, G. M. *SHELXS-97, Program for Crystal Structure Refinement*; University of Göttingen: Germany, 1997.
(19) Sheldrick, G. M. *SHELXL-97, Program for Determination of Crystal Structures*; University of Göttingen: Germany, 1997.
(20) Details may be obtained from Fachinformationszentrum Karlsruhe, D-76344 Eggenstein-Leopoldshafen (Germany), by quoting the Registry No. CSD-414513. E-mail: crysdata@fiz-karlsruhe.de.
(21) (a) Blöchl, P. E. *Phys. Rev. B* **1994**, *50*, 17953. (b) Kresse, G.; Joubert, J. *Phys. Rev. B* **1999**, *59*, 1758.
(22) Kresse, G.; Hafner J. *Phys. Rev. B* **1993**, *47*, 558. (b) Kresse, G.; Furthmüller J. *Phys. Rev. B* **1996**, *54*, 11169.
(23) Ceperley, D. M.; Alder, B. J. *Phys. Rev. Lett.* **1980**, *45*, 566.
(24) Monkhurst, H. J.; Pack, J. D. *Phys. Rev. B* **1978**, *13*, 5188.
(25) Krier, G.; Jepsen, O.; Burkhardt, A.; Andersen, O. K. *The TB-LMTO-ASA Program*, Version 4.7; Max-Planck Institut: Stuttgart, Germany, 1997.
(26) Dronskowski, R.; Blöchl, P. E. *J. Phys. Chem.* **1993**, *97*, 8617.
(27) Häussermann, U.; Landa-Cánovas, A.; Lidin, S. *Inorg. Chem.* **1997**, *36*, 4307.

Table 4. Atomic Coordinates and Isotropic Displacement Parameter (pm²) for $Li_{1.42(5)}Pd_2Sn_{5.58(5)}$ (space group *P4/mbm*)[a]

atom	Wyckoff position	occup./%	*x*	*y*	*z*	U_{eq}/U_{iso}
Li1	4*a*	100	0	0	1/2	209(29)
Pd	4*e*	100	0	0	0.18035(4)	139(1)
Sn1	8*k*	100	0.65777(3)	1/2+x	0.31913(3)	147(1)
Sn2/Li2	4*h*	79.0(1)/21.0(1)	0.83690(5)	1/2+x	0	151(1)

[a] U_{eq} is defined as one-third of the trace of the orthogonalized U_{ij} tensor.

Table 5. Interatomic Distances (pm) of $Li_{1.42(5)}Pd_2Sn_{5.58(5)}$, Calculated with the Lattice Parameters Taken from X-ray Powder Data[a]

Li1:	2	Pd	269.6	Pd:	1	Li1	269.6
	8	Sn1	292.6		4	Sn1	275.8
Sn1:	2	Pd	275.8		4	M	290.9
	2	Li1	292.6		1	Pd	304.2
	1	Sn1	295.7	*M*:	4	Pd	290.9
	1	Sn1	305.1		1	M	305.7
	1	M	317.2		2	Sn1	317.2
	2	M	343.0		4	Sn1	343.0
	4	Sn1	353.1		4	M	350.8

[a] The *M* site shows mixed tin/lithium occupancy (see Table 4). All distances within the first coordination spheres are listed. Standard deviations are all equal to or smaller than 0.1 pm.

the *a* parameter is about 15 pm larger than the *b* and *c* parameter of $PdSn_3$. On the other hand the repeat of the Pd_2Sn_6 building block in $Li_{1.42(5)}Pd_2Sn_{5.58(5)}$ (i.e., the *c* parameter) is 14 pm smaller than in $PdSn_3$ (*a*/2). Due to these changes, the width of the Pd_2Sn_6 blocks of 538 pm in $Li_{1.42(5)}Pd_2Sn_{5.58(5)}$ is also smaller than that in $PdSn_3$ (578 pm).

Although these geometrical parameters differ drastically, interatomic Pd−Sn and Sn−Sn distances are very similar in both compounds: Pd−Sn distances in $PdSn_3$ and $Li_{1.42(5)}Pd_2Sn_{5.58(5)}$ range from 279 to 284 pm and 276 to 291 pm, respectively, and are thus slightly longer than the sum of the covalent radii of 268 pm.[28] Sn−Sn distances cover the ranges 294−345 pm in $PdSn_3$ and 296−353 pm in $Li_{1.42(5)}Pd_2Sn_{5.58(5)}$. A small, but decisive difference between the two structures is noted for the Pd−Pd distance within Pd_2Sn_6 building blocks. In the intercalated compound this distance is considerably larger compared to that of $PdSn_3$ (304 vs 293 pm). The increase is reverse to the smaller building block width and repeat in $Li_{1.42(5)}Pd_2Sn_{5.58(5)}$ and places the Pd atoms considerably off the center of their square antiprismatic coordination polyhedra. It could be suspected that this structural difference is a consequence of the mixed Sn2/Li2 occupancy of the 4*h* site in $Li_{1.42(5)}Pd_2Sn_{5.58(5)}$, i.e., smaller Pd−Sn1 distances of 276 pm and longer Pd−Li2/Sn2 distances of 291 pm.

The central question is why a stannide with the ideal composition $LiPd_2Sn_6$ has not been observed. This seems to be a question of the valence electron concentration. The block Pd_2Sn_6 has an electron count of 44 (2 × 10 + 6 × 4), while the electron count of $LiPd_2Sn_6$ is 45 (1 × 1 + 2 × 10 + 6 × 4). If we consider the electron count of 44 as an optimum for $PdSn_3$, the ideal composition $LiPd_2Sn_6$ would be destabilized by the higher electron count of 45. The $Li_{1.42(5)}Pd_2Sn_{5.58(5)}$ structure is stabilized through the mixed Sn2/Li2 occupancy, leading to an electron count of 43.7 for $Li_{1.42(5)}Pd_2Sn_{5.59(5)}$ (1.42 × 1 + 2 × 10 +5.58 × 4). This simple electron counting scheme readily explains why all the crystals investigated have almost the same composition,

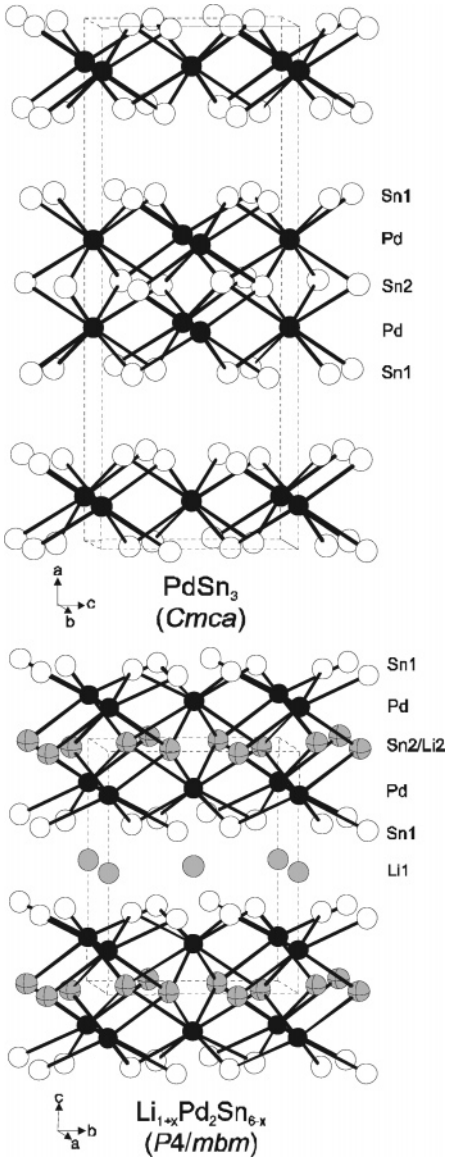

Figure 1. Crystal structures of $PdSn_3$ and $Li_{1+x}Pd_2Sn_{6-x}$. The two-dimensional $[Pd_2Sn_6]$ networks are emphasized.

leading to electron counts around 44. The peculiar situation of chemical bonding in $Li_{1+x}Pd_2Sn_{6-x}$ has been further elucidated by electronic structure calculations.

Chemical Bonding. Total energy calculations were performed for $LiPd_2Sn_6$ in the experimentally determined structure type of $Li_{1.42(5)}Pd_2Sn_{5.58(5)}$. As a first step the structural parameters and volume of this idealized compound were computationally relaxed and the result is summarized in Table 6. It can be noted that the positional parameters of computational $LiPd_2Sn_6$ and experimental $Li_{1.42(5)}Pd_2Sn_{5.58(5)}$ are rather close (somewhat surprising, the largest deviation occurs for the *z* parameter of the Pd 4*e* position and not for the *x* parameter of the mixed occupied 4*h* site), whereas the

(28) Emsley, J. *The Elements*; Oxford University Press: Oxford, U.K., 1999.

Table 6. Structural Parameters of Computationally Relaxed $LiPd_2Sn_6$ (Space Group *P4/mbm*)[a]

atom	Wyckoff position	x	y	z
Li1	4*a*	0	0	1/2
Pd	4*e*	0	0	0.1782
Sn1	8*k*	0.6588	1/2+x	0.3214
Sn2	4*h*	0.8369	1/2+x	0

[a] $a = 656.87$ pm, $c = 853.96$ pm, $c/a = 1.30$, $V = 0.368$ nm^3.

Table 7. Comparison of Interatomic Distances (pm) in Computationally Relaxed $PdSn_3$ and $LiPd_2Sn_6$

$PdSn_3$				$LiPd_2Sn_6$			
				Li:	2	Pd	275
					8	Sn1	290
Pd:	2	Sn1	276	Pd:	1	Li	275
	2	Sn1	278		4	Sn1	276
	2	Sn2	280		4	Sn2	289
	2	Sn2	281		1	Pd	304
	1	Pd	289				
Sn1:	1	Pd	276	Sn1:	2	Pd	276
	1	Pd	278		2	Li	290
	1	Sn1	296		1	Sn1	295
	1	Sn1	307		1	Sn1	305
	1	Sn2	325		1	Sn2	321
	2	Sn1	335		2	Sn2	347
	2	Sn1	338		4	Sn1	350
Sn2:	2	Pd	280	Sn2:	4	Pd	289
	2	Pd	281		1	Sn2	303
	1	Sn2	291		2	Sn1	321
	2	Sn1	325		4	Sn1	347
	2	Sn2	338		4	Sn2	348
	2	Sn2	342				

axial ratios differ considerably. The comparison of the theoretical equilibrium structure of $LiPd_2Sn_6$ with that of $PdSn_3$ structure gives an unbiased opportunity to view the effect of Li insertion to crystal and electronic structure. For $PdSn_3$ we previously observed that our calculational method very well reproduced the experimental structure,[6] apart from a slight underestimation of the volume by 3.5%. This overbinding is typical of the applied LDA approximation.

When reasonably assuming that the idealized structure of $LiPd_2Sn_6$ is equally well reproduced by theory the most prominent direct effect of Li insertion in $PdSn_3$ becomes immediatley apparent. Apart from the expected altered stacking sequence of building blocks, Pd atoms within these double layers of square antiprisms are moved toward the inserting Li atoms. This elongates the Pd−Pd distance from 293 to 304 pm and shifts the Pd atoms off the center of their Sn square antiprismatic coordination polyhedron (Table 7). This important effect also seen in the experimental structure of $Li_{1.42(5)}Pd_2Sn_{5.58(5)}$ is therefore not connected to the mixed occupied position, but rather a consequence of Pd−Li interactions. Conversely the considerably decreased stacking repeat of the Pd_2Sn_6 building blocks in $Li_{1.42(5)}Pd_2Sn_{5.58(5)}$ compared to $PdSn_3$ is not observed when comparing the computationally relaxed structures: the values of the *c* parameter of $LiPd_2Sn_6$ (853.96 pm) and *a*/2 of $PdSn_3$ (857.35 pm) are about the same. This decrease has to be a consequence of the mixed occupied position Sn2/Li2. Further, it can be noted that the introduction of Li in $PdSn_3$ is notably exothermic. The calculated formation energy (referring to zero Kelvin) for the reaction $Li + 2\ PdSn_3 = LiPd_2Sn_6$ is −0.86 eV/Z (−80 kJ/mol).

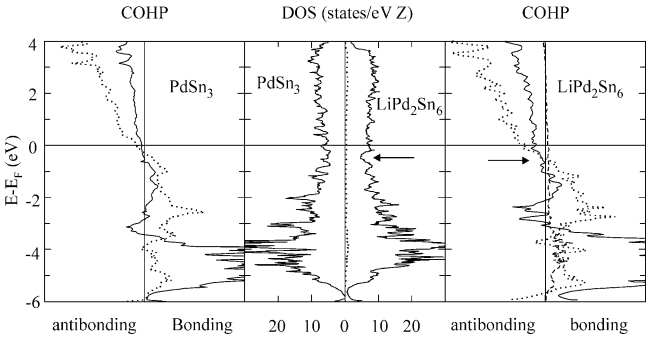

Figure 2. Total DOS (middle panel) for the stannides $PdSn_3$ and $LiPd_2Sn_6$ calculated at the theoretical equilibrium volume. For the latter system the partial DOS of the Li site is drawn with the dotted line. The arrow marks a dip in the DOS for $LiPd_2Sn_6$ corresponding to an electron count of 43.4 e/Z. The left and right panels show COHP summed for all Pd−Sn (solid line) and Sn−Sn contacts (dotted line) in the unit cell below 350 pm for $PdSn_3$ and $LiPd_2Sn_6$, respectively. Additionally, the right panel shows COHP for the Li−Pd and Li−Sn contacts (broken line). The arrow in the right panel marks the turnover point of the Pd−Sn and Sn−Sn contacts from bonding/nonbonding to antibonding. The Fermi level E_F is set to zero.

The result of the electronic structure analysis of $PdSn_3$ and $LiPd_2Sn_6$ is compiled in Figure 2. It can be seen that the electronic density of states (DOS) of both compounds is virtually identical. Li based states in $LiPd_2Sn_6$ are rather equally distributed over a large energy range below and above the Fermi level. For $PdSn_3$ the Fermi level separates quite well Pd−Sn and Sn−Sn bonding/nonbonding from antibonding states. For $LiPd_2Sn_6$, however, the change of bonding character occurs at about −0.5 eV below the Fermi level. Interestingly, this energy coincides with a small dip in the DOS of $LiPd_2Sn_6$, which is the only noteworthy difference between the DOS of $PdSn_3$ and $LiPd_2Sn_6$. When the Fermi level is shifted to this dip 43.4 electrons per formula unit can be accommodated. This value is close to the electron count of 43.7 extracted from the experimental composition $Li_{1.42(5)}Pd_2Sn_{5.58(5)}$. To summarize, the incorporation of Li in $PdSn_3$ creates a small dip in the DOS slightly below the Fermi level. The location of the dip coincides with the energy where the bonding character of the primary interactions (Pd−Sn and Sn−Sn) changes in $LiPd_2Sn_6$. Thus, reduction of the electron count in $LiPd_2Sn_6$ would optimize the bonding situation in this system. One way to achieve this is the replacement of a small amount of Sn by the more electron poor Li and thus introducing a mixed occupied Sn/Li position. This is experimentally observed.

Acknowledgment. We thank H.-J. Göcke for the work at the scanning electron microscope, B. Heying and Dipl.-Ing. U. Ch. Rodewald for collection of the diffractometer data, and the Degussa-Hüls AG for a generous gift of palladium powder. Financial support by the Deutsche Forschungsgemeinschaft through SFB 458 "Ionenbewegung in Materialien mit ungeordneten Strukturen" is gratefully acknowledged. P.S. is indebted to the NRW Graduate School of Chemistry for a PhD stipend.

CM0401995